Journal of Colloid and Interface Science 693 (2025) 137572

Contents lists available at ScienceDirect

Journal of Colloid And Interface Science

journal homepage: www.elsevier.com/locate/jcis

Regular Article

# Balance of hydrophobic and electrostatic interaction of polymers and surfactants: Case of anionic surfactant and hydrophobically modified polymer

Egor A. Bersenev [a,b,*], Lauren Matthews [a,1], Valentina Rein [a], Rebecca J. Fong [c], Oleg V. Konovalov [a], Wuge H. Briscoe [b,*]

[a] European Synchrotron Radiation Facility (ESRF), 71 avenue des Martyrs, Grenoble, 38000, France
[b] School of Chemistry, University of Bristol, Cantock's Close, Bristol, BS8 1TS, United Kingdom
[c] Procter&Gamble, Newcastle Innovation Centre, Newcastle upon Tyne, NE12 9TS, United Kingdom

## GRAPHICAL ABSTRACT

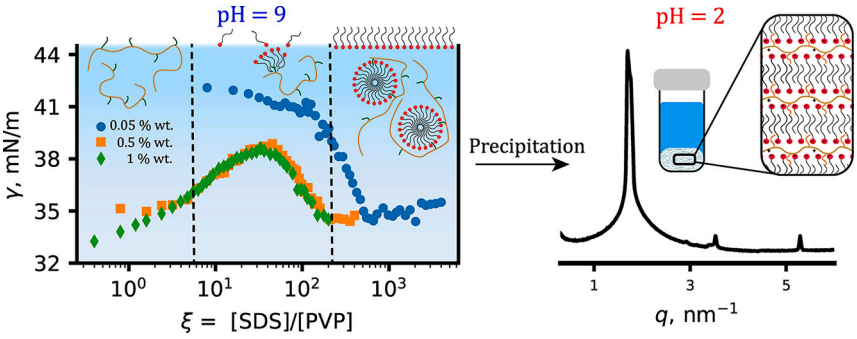


## ABSTRACT

We investigated the structure of polymer-surfactant aggregates and their pH-dependent structural evolution using hydrophobically modified poly(vinyl-pyrrolidone) (h-PVP) and sodium dodecyl sulfate (SDS). The structure of the complexes in the weak (pH ≃ 9) and strong (pH ≃ 2) interaction regimes was studied using small-angle X-ray scattering, with the data analysed on an absolute intensity scale, using molecular parameters as constraints. At pH 9, where self-assembly was driven by hydrophobic interactions, we have found that, at low surfactant concentrations, elongated aggregates were formed. At excess surfactant concentrations, the aggregates became more compact with a smaller aggregation number, resembling free micelles with the hydrophobic domains of the polymer incorporated into the surfactant core. In all cases, aggregates formed a continuous network, with polymer serving as a weak cross-linker between aggregates. Finally, we have compared the structure of these weakly interacting aggregates with the precipitates formed at low pH, where the electrostatic attraction dominates.

* Corresponding authors.
*E-mail addresses:* egor.bersenev@bristol.ac.uk (E.A. Bersenev), wuge.briscoe@bristol.ac.uk (W.H. Briscoe).
[1] Present address: ISIS Neutron and Muon Source, Rutherford Appleton Laboratory, Chilton, OX11 0QX, UK.

https://doi.org/10.1016/j.jcis.2025.137572
Received 29 November 2024; Received in revised form 7 April 2025; Accepted 10 April 2025
Available online 14 April 2025

## 1. Introduction

Interactions between polymers and surfactants, both in solution [1,2] and at interfaces [3], have been extensively studied due to their high industrial and scientific relevance. Polymer-surfactant complexes are widespread in consumer products and biomedical applications [4,5], e.g. as thickening agents in cosmetics [6] and as foam stabilizers for topical drug delivery [7,8]. Such interactions depend intricately on the polymer molecular weight, architecture, charge density, and amphiphilicity. [6,9] Polyelectrolytes containing hydrophobically modified moieties are of particular interest due to their desirable properties as additives in personal care products, e.g. reduced irritation [10] beneficial for skin-friendly cleansers and "no-tears" shampoo formulations [11].

Driven by electrostatic and hydrophobic forces and entropic effects, polymers and surfactants can assemble into supramolecular complexes (P-S complexes) above a certain concentration, often referred to as the *critical association concentration* (cac) [12,13]. These interactions can be rationalized by two different models. In the *closed association model*, surfactants bind to the polymer, forming micelle-like aggregates in the vicinity of the polymer chain. This leads to a relatively large number of surfactant molecules distributed unevenly on the chain in aggregates. In the *site binding model* (the Zimm-Bragg theory) [14], surfactants are bound as ions to the oppositely charged polymer segments, leading to a relatively even distribution of surfactants along the polymer chain. There is a longstanding debate in the literature about the mechanism of the binding process between polymers and surfactants.

In practical applications, P-S complex stability is an important consideration, as the presence of large non-equilibrium aggregates can significantly alter the properties of the mixtures [15,16], leading to the loss of product properties. P-S complexation is underpinned by polymer-surfactant interactions. Upon approaching stoichiometric binding between polyelectrolytes and ionic surfactants, diminishing long-range electrostatic repulsion can lead to aggregation of complexes and precipitation, and subsequent macroscopic phase separation. This process may take significant time, up to several months [17,18]. To avoid precipitate formation, one approach is to manipulate the charge density of the surfactant aggregates by incorporating non-ionic surfactants [19–21]. There have also been attempts to incorporate responsive components, making it sensitive to pH, temperature, UV-light and other external stimuli [22,23].

Up to now, most previous work has focused on the oppositely charged P-S structure either at interfaces [17,24,25] or in solution. In many of these studies, the solution structure was affected by the presence of out-of-equilibrium aggregates formed due to the strong electrostatic interaction between the components, which depended sensitively on sample preparation, requiring complex protocols. [26–28] As a consequence, it is challenging to experimentally obtain equilibrium P-S complexes and few studies have examined the connection between the P-S complex interfacial behaviour and their aggregate structure in solution. Therefore, the mechanistic insight into the structure of P-S aggregates at equilibrium is limited. Equilibrium P-S complexes may be attained by controlling the interaction between components, e.g. by tuning polymer charge density. For instance, P-S complexes with pH responsive polymers have been studied [29–31], but understanding of how the polymer charge tunability affects surfactant binding and the complex structure remains incomplete.

Interaction of sodium dodecyl sulfate (SDS) and poly (vinylpyrrolidone) (PVP) has been studied at the interface using surface tension measurements [32,33] and neutron reflectometry (NR) [32]; and in solution using microcalorimetry [34], conductometry [33], capillary electrophoresis [35,36], NMR [37], and small-angle neutron scattering (SANS) [38,39], as well as theoretically. [40] An NR study of the interfacial interaction between PVP and SDS [32] attributed lowering in the surface tension to the possible formation of polymer-surfactant complexes in the bulk, although direct experimental evidence was not provided. Capillary electrophoresis results suggested the formation of a pseudo-polyanion due to the PVP-SDS interaction, pointing to the role of ion bridging in the complex formation. [41] Results from NMR investigation [37] suggested strong specific interactions between the SDS headgroups and PVP, which restricted the mobility of water molecules in the headgroup region, although it was not attempted to vary the strength of this interaction through manipulation of the ionic strength or pH. Furthermore, a SANS investigation of the aggregate structure [38,39] focused on a single polymer concentration, showing the localisation of polymer around surfactant headgroups. Despite these previous studies of the SDS-PVP interaction, it remains under-explored how the interaction strength might be tuned e.g. *via* pH variation, which would also facilitate obtaining equilibrium P-S complexes, allowing a direct comparison with P-S precipitates.

Here, the structure of P-S complexes in solution with the driving force switchable between hydrophobic and electrostatic interactions has been investigated, enabled by use of a hydrophobically modified pH-responsive polyelectrolyte. The co-polymer consists of a statistical distribution of pH responsive polyvinylpyrrolidone (PVP) and hydrophobic butyl segments. It is uncharged at pH = 9 (greater than PVP pKa = 8.3 [42]) where its interaction with anionic surfactant sodium dodecyl sulfate (SDS) is dominated by the hydrophobic interaction. At pH = 2, PVP is positively charged and forms precipitates with SDS due to strong electrostatic interactions. This experimental system thus allows us to directly compare the P-S complex structure, with the same composition but different driving forces. The complex structure has been studied using small-angle X-ray scattering (SAXS), complemented by equilibrium surface tension measurements, which allowed the proposition of a structural model of polymer-surfactant interaction, facilitating mechanistic insights into surfactant binding to the polymer.

## 2. Materials and methods

### 2.1. Materials

Butylated polyvinylpyrrolidone (h-PVP, Ashland Surfaguard AL-9) with a molar mass $M_n = 8 - 12\,\mathrm{kg \cdot mol^{-1}}$, $M_w = 30 - 50\,\mathrm{kg \cdot mol^{-1}}$ was provided by Procter & Gamble, UK, and used as received. $^1$H NMR measurement was conducted to confirm the copolymer structure. (cf. Supplementary material S4) Ethanolamine (product number E9508, $\geq 98\%$) and sodium dodecyl sulfate (SDS; product number L4509, $\geq 98.5\%$) were purchased from Sigma and used as received. Ultrapure Milli-Q water (Resistivity = $18.2\,\mathrm{M\Omega \cdot cm}$ and total organic content (TOC) = 2 ppb) was used to prepare all aqueous solutions.

### 2.2. Sample preparation

Samples were prepared by mixing stock solutions of the components in Eppendorf test tubes, which were shaken at 35 $^o$C for 30 minutes in a thermal mixer and then stored at room temperature for 2 weeks before further use. The sample composition for all samples is provided in the supplementary material, Section S10.

Precipitates of the h-PVP and SDS mixture at pH 2 were prepared by dropwise addition of the 1 M solution of hydrochloric acid to the beaker containing 10 mL of 50 mM SDS and 1 wt% of h-PVP under vigorous stirring. The solution was let to equilibrate for 7 days at room temperature, before being centrifuged for 30 minutes at 8000 rpm. Sedimented viscoelastic film was collected and transferred into SAXS gel cells in excess of water for measurements.

### 2.3. Small-angle X-ray scattering (SAXS)

SAXS measurements were carried out on the ID02 beamline at the European Synchrotron Radiation Facility (ESRF) in Grenoble, France [43]. The experiments were conducted in transmission geometry using a photon energy of 12.23 keV, corresponding to a wavelength, $\lambda$ = 0.1 nm. Measurements were performed with a pixel array detector,

Eiger2 4M (Dectris Ltd., Switzerland), at a 0.8 and 10 meter sample-to-detector distance, covering a $q$-range of 0.006 — 10 $nm^{-1}$. Static SAXS measurements were carried out in a flow-through capillary setup, with a capillary diameter of 2 mm, in combination with a 28-port automated sample changer, with transmission measured simultaneously. Radiation damage was checked by making a series of test exposures, and only the data that showed no radiation damage were further analysed. The recorded 2D data were normalised to an absolute intensity scale before regrouping to obtain the 1D SAXS profiles. The corresponding background was then subtracted from each of the 1D profiles. The obtained dataset is available at the ESRF repository [44].

Measurements of the scattering from the precipitates were conducted on the BM26 beamline at ESRF in transmission geometry using a photon energy of 12.4 keV ($\lambda = 0.1$ nm) and a pixel array detector, Pilatus 1M (Dectris Ltd., Switzerland) with a 1 meter sample-to-detector distance, covering a $q$-range of 0.2 — 8 $nm^{-1}$. Samples were loaded into gel cells with mica windows and exposed to X-rays for 10 s. The recorded 2D data were normalized by transmission, with background subtracted, and regrouped to obtain 1D SAXS profiles.

### 2.4. Surface tension measurements

Equilibrium surface tension measurements were conducted using a Krüss K11 force tensiometer equipped with a Wilhelmy plate. Before each measurement, the glass vessel was cleaned with hot water, rinsed with pure ethanol and Milli-Q water, and the platinum Wilhelmy plate was cleaned in the flame of a Bunsen burner. Subsequently, cleanliness was checked by measuring the surface tension of Milli-Q water to ensure the absence of any surface active molecules.

Titration experiments were conducted by adding a mixed polymer/surfactant solution into the polymer solution of a designated concentration, therefore achieving a constant polymer concentration with varying surfactant concentrations. After each addition, samples were vigorously stirred for 1 min and then allowed to equilibrate for at least 5 min before measurement.

Then, the tensiometer was allowed to equilibrate, until the fluctuations in the reading of the weight sensor were $< 0.025$ g. After that, a measurement was started with the following procedure: the weight sensor was tared to 0, after that surface was automatically detected and Wilhelmy plate was submerged 2 mm into the liquid. Sensor readings were recorded every 30 seconds, until a plateau was reached with the standard deviation of the last 10 readings $< 0.01\ mN \cdot m^{-1}$. This process allowed us to ensure that the surface has reached equilibrium.

## 3. Results and discussion

### 3.1. Surface activity of the polymer

With $\sim 10\%$ of the copolymer units being hydrophobic grafts and $M_w \simeq 40000\,g/mol$, the number of repeat monomer units is estimated as $N = 370$, with a contour length of 94 nm with the hydrophobic grafts 10 nm apart. Structure of the h-PVP polymer is shown in the inset of the Fig. 1. Characterisation of the hydrophobically modified PVP has not been previously reported. Equilibrium surface tension ($\gamma$) of the polymer is plotted as a function of its concentration ($c_{PVP}$) in Fig. 1, showing significant lowering of $\gamma$ compared to that of pure water at a polymer concentration as low as $c_{PVP} \simeq 10$ ppm.

The hydrophobic butyl grafts along the PVP backbone facilitate interfacial activity, leading to adsorption of the polymer to the air-water interface, effectively reducing the surface tension. At higher concentrations it would also lead to self-aggregation into micelle-like structures. This behaviour is a common feature of hydrophobically modified polymers [45], including the presence of a well-defined *cac* which depends on the polymer architecture, i.e. the density and length of the hydrophobic grafts and other parameters. [46,47] Non-modified PVP is known to have little surface activity, even at concentration of 10 000 ppm (1% wt) [48,49].

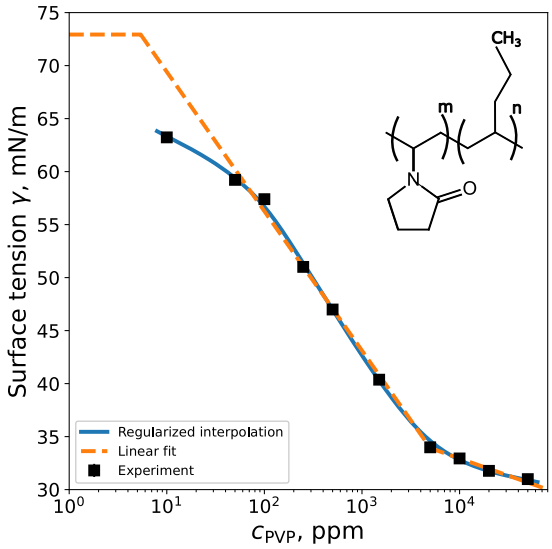


**Fig. 1.** Surface tension of aqueous PVP solution plotted vs PVP concentration, $c_{PVP}$. Black squares are data points. Error bars are smaller than symbol size. Solid blue line indicates regularised spline interpolation of the data. The plateau in the dashed orange line corresponds to the surface tension of pure MilliQ water, with the straight section the linear fit to the data points between 100 and 1500 ppm, followed by a further linear fit of the data points above 5000 ppm. Intersection of the line with the $\gamma_{MilliQ}$ occurs at $c_{PVP} = 5.8 \pm 0.2$ ppm, and the intersection of the two linear fits occurs at $c_{PVP} = 5015 \pm 576$ ppm. Inset shows the chemical structure of the h-PVP polymer.

Whilst a hydrophobically modified polymer solution cannot be treated as a dilute surfactant solution [50], it is useful to estimate the surface excess $\Gamma$ of the polymer at the air-water interface using the Gibbs adsorption isotherm analysis:

$$\Gamma = -\frac{1}{iRT} \cdot \left( \frac{d\gamma}{d \ln c} \right)_{P,T} \quad (1)$$

where $R$ is the gas constant, $T$ the absolute temperature, and $i$ corresponds to the activity coefficient which in the case of non-ionic species is equal to 1. Above a certain concentration $c_{lim}$, the calculated surface excess reaches a maximum, which can be regarded as the point where the Gibbs isotherm requires the inclusion of a self-aggregation term [50]. Using the equation we can estimate the limit of the validity of the extensive approximation as $c_{lim} = 500$ ppm, with the corresponding $\Gamma$ vs $c_{PVP}$ plot (cf. Supplementary material, Figure S1). Accordingly, three PVP concentrations were chosen, i.e. $c_{PVP} = 500, 5000,$ and 10000 ppm, corresponding respectively to the beginning of polymer aggregation, *cac*, and higher polymer concentration where self-organized aggregates are prominent.

### 3.2. Interaction of the polymer with surfactant at pH = 9: impact on surface tension

At pH 9, PVP is uncharged ($pK_\alpha = 7.5$ [42]), with the P-S complex structure at the interface and in the solution dominated by hydrophobic interactions, and no precipitation occurs. Fig. 2 shows the equilibrium surface tension $\gamma$ of the polymer-surfactant mixture vs the SDS concentration [SDS] at three PVP concentrations, i.e. $c_{pvp} = 500$, 5000, and 10000 ppm, respectively, at pH = 9. The inset shows $\gamma$ vs the SDS-PVP molar concentration ratio, $\xi$ = [SDS] / [PVP]. Due to the high surface activity of the PVP, surface tension exhibited low values ($\gamma < 45\ mN \cdot m^{-1}$) over the wide range of SDS concentrations. The $c^{cmc}_{SDS} = 8$ mM of pure SDS solution is indicated with a dotted line in Fig. 2, with the full SDS surface tension isotherm shown in Figure S2.

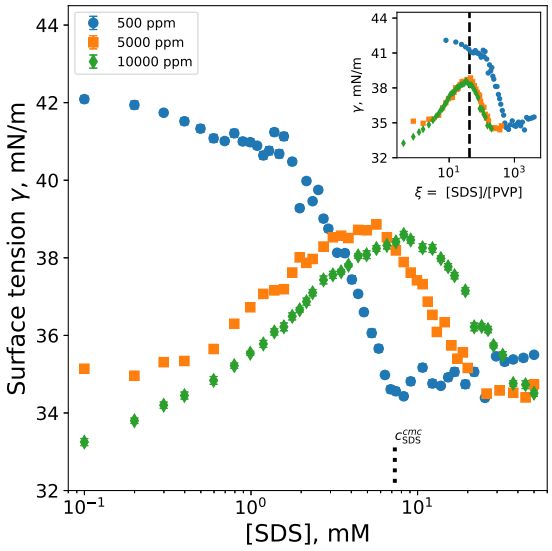


**Fig. 2.** Surface tension of the PVP/SDS complexes plotted vs SDS concentration with the PVP concentration of $c_{PVP}$ = 500 ppm, 5000 ppm and 10000 ppm. Dotted line indicated the *cmc* of SDS. Inset shows the same curves but plotted vs SDS/PVP molar ratio $\xi$. Dashed vertical line indicated the $c_{cac}$ at which saturation of polymer chains occurs.

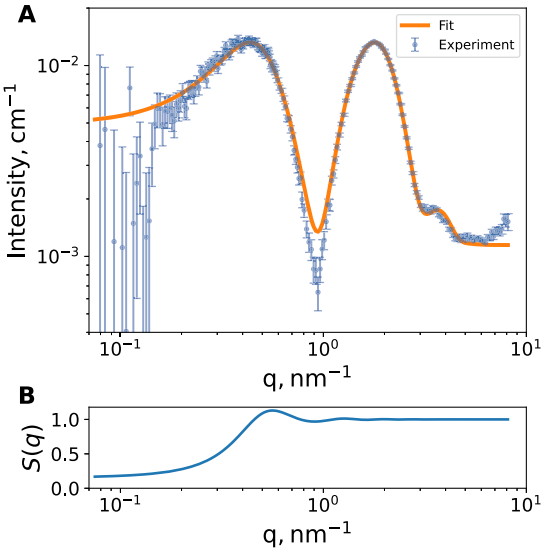


**Fig. 3.** A. SAXS intensity vs scattering vector modulus, q, in 50mM SDS solution, with the solid line the fit using the ellipsoidal core-shell model with a Hayter-Penfold structure factor $S(q)$ shown in B.

At $c_{pvp}$ = 500 ppm, $\gamma$ decreased gradually from 42 mN · m$^{-1}$ slightly to 41 mN · m$^{-1}$ at [SDS] = 0.5 mM, followed by a sharp drop to 34 mN · m$^{-1}$ at [SDS] = 8 mM which indicates SDS micellization.

Surface tension $\gamma$ for the pure polymer solution at $c_{pvp}$ = 5000 and 10000 ppm without SDS exhibited low values, i.e. $\gamma$ = 35 mN · m$^{-1}$ and 33 mN · m$^{-1}$, respectively. Upon SDS addition, the surface tension initially increased before peaking at $\gamma \simeq 39$ mN · m$^{-1}$ for both polymer concentrations. The corresponding SDS concentration is the critical association concentration, $c_{cac}$, at which complexation of surfactant with the polymer would be completed, the value of which depends on the polymer concentration, i.e. $c_{cac}^{0.5\%} = 5.3$ mM for $c_{PVP}$ = 5000 ppm and $c_{cac}^{1\%} = 10.5$ mM for $c_{PVP}$ = 10000 ppm, respectively. As proposed by Shinoda [51], $c_{cac}$ should be a function of only the surfactant-to-polymer ratio $\xi$. Using the polymer molar mass, it is possible to estimate the number of SDS molecules per PVP chain, $\xi_{cac} = N_{agg} = 43$, at the maximum surface tension, as indicated by the dashed line in the $\gamma$ vs $\xi$ plot in the inset of Fig. 2, consistent with Shinoda's prediction.

Further increase in the SDS concentration led to a decrease in the surface tension for both $c_{pvp}$ = 5000 and 10000 ppm which was followed by a plateau at $\gamma = 34$ mN · m$^{-1}$. This value is similar to that of the surface tension of pure SDS solution above its cmc. The change in the surface tension over the range of SDS concentrations is small ($\Delta\gamma < 5$ mN · m$^{-1}$) in magnitude, compared to the pure SDS solution (cf. Supplementary material, Figure S2) with $\Delta\gamma > 40$ mN · m$^{-1}$, which indicates that surfactant binding did not lead to the depletion of the adsorbed layer. Rather, it consisted of both polymer moieties and surfactant molecules, which is in line with the observations of Penfold et al. [52]

However, the composition of the interfacial layer changed with the SDS concentration, evident from the surface tension evolution. This could be attributed to the cooperative adsorption of the neutral polymer and the surfactant at low SDS concentrations, i.e. $c_{SDS} < 1$ mM, in the presence of 10000 ppm of PVP and transition to the competition regime at higher surfactant concentrations indicated by an increase in surface tension. This is followed by the displacement of the polymer from the surface after the association process is completed, as was demonstrated by Slastanova et al. [53,54] using a combination of surface tension measurements and neutron reflectivity (NR). There were other attempts to quantify the composition of the interfacial layer through the variation of the isotopic contrast [32,55–57]. It was observed that PVP/SDS adsorbed on the interface mostly in the form of a complex, which formed at low concentration and was largely responsible for the surface tension reduction, although the structure of solution aggregates was not reported.

### 3.3. Structure of pure SDS micelles and polymer chains in aqueous solution from SAXS

Figs. 3 and 4 show the SAXS curves from the solutions of the surfactant and polymer, respectively. For SAXS curve at $c_{SDS}$ = 50 mM, above its cmc (Fig. 3), SDS micelles were modelled as monodisperse prolate ellipsoids with a minor axis $a = 13.7$ Å and a core eccentricity of $\epsilon_{core} = 1.62$. The fitted shell thickness $T_{shell} = 9.4$ Å is higher than the literature value of $T_{shell} = 5.45$ Å [58] in buffer, although it is in line with the observation in pure water and where the extended q-range was taken into account [59]. Confidence intervals were estimated from the posterior distributions, obtained by the Markov-Chain Monte-Carlo sampling. (cf. Supplementary material, Section S9) From the fitting, the micelle aggregation number was determined to be $n_{agg} = 49$. Analysis of the structure factor, plotted in the Fig. 3B, yields the effective charge $q_{eff} = 14\,e^-$ per micelle, which corresponds to an SDS degree of dissociation $\beta = 29\%$. The results are in good agreement with the observation by Bergstrom et al. [60], where for 1 wt% solution and $n_{agg} = 60$ the degree of dissociation was calculated to be 26% at 40$^o$ C. The discrepancy between the calculated and measured intensity at $q = 1$ nm$^{-1}$ is attributed to the use of the biaxial ellipsoid model. The fit can be improved by use of the triaxial ellipsoid model (for comparison cf. S11) or a molecular dynamic simulations for calculation of the SAXS intensity. [59] However, inclusion of another parameter is not fully justified for the modelling of scattering from the P-S complexes, so we have decided to use a simple model of a biaxial core-shell ellipsoid for the description of the scattering from the pure micellar solution of SDS.

Fig. 4A shows the SAXS curves in the PVP solution at different concentrations, i.e. $c_{pvp}$ = 500 ppm (0.05 wt%), 5000 ppm (0.5 wt%), and 10000 ppm (1 wt%), and the solid lines represent the fits using the Gaussian chain model with excluded volume effects, as described in [61] with the fitting parameters (radius of gyration $R_g$, Flory exponent $\nu$, and forward scattering intensity $I_0^p$ are shown in Fig. 4B, C, and D, respectively). The estimated overlap concentration is $c^* = 7500$ ppm, therefore only the 10 000 ppm solution was in the semi-dilute regime. A more detailed description of the model and $c^*$ calculation can be found in the Supplementary material, section S5 and S8, respectively.

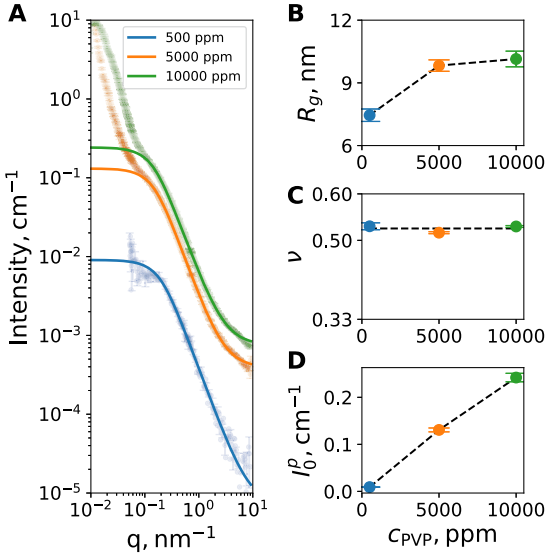


**Fig. 4.** A. SAXS intensity I vs scattering vector modulus, q, for $c_{PVP}$ = 500, 5000 and 10000 ppm. Solid lines indicate fits to the model; B. Radius of gyration $R_g$; C. Flory exponent $\nu$, and D. Forward scattering intensity $I_0^p$, vs the polymer concentration $c_{PVP}$, with the dashed line a guide to the eye. Error bars are comparable to, or smaller than, the data symbol size, with the error values listed in Table S7.

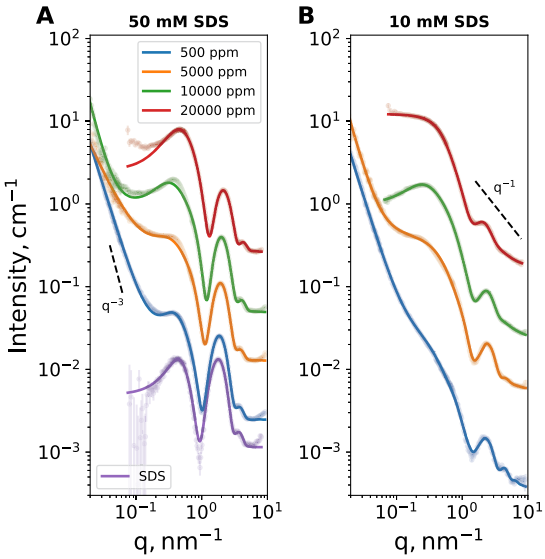


**Fig. 5.** A. SAXS intensity, I, as a function of scattering vector modulus, q, for $c_{PVP}$ = 500, 5000, 10000, and 20000 ppm with 50 mM of SDS and B. 10 mM of SDS. The SAXS curve in the pure 50 mM SDS micellar solution is also included for comparison in A. The intensity is re-scaled by a factor of 3 consecutively for the SAXS curves for clarity.

The low-q upturn in the scattering curve is fitted with a mass fractal model [62] with the fitted $R_g$ of individual chains in the range of 6-10 nm and the fitted aggregate size 160-200 nm, which is consistent the DLS hydrodynamic radius $R_h$ = 60-80 nm [63] (cf. Supplementary material, Section S14). The Flory exponent $\nu = 0.53$, shown in the Fig. 4C, does not depend on the polymer concentration. Kamli et al. [64] reported a value of $\nu$ = 0.55 in pure water, a good solvent for PVP, in good agreement with our observations. This indicates that the solubility of PVP segments was not significantly modified by the presence of hydrophobic grafts. Aggregation of PVP chains can occur even for a non-modified polymer, due to the effect of hydrogen bonding in the semi-dilute regime, as demonstrated previously [65]. In our work, the aggregation of h-PVP is primarily driven by the incompatibility of the butyl grafts with water. Overall, it appears that, under the conditions in this work, water acted as a close-to-theta-solvent for h-PVP.

### *3.4. Structure of polymer-surfactant complexes in solution at pH = 9 from SAXS*

The SAXS curves for complexes with different polymer concentration at $c_{SDS}$ = 50 and 10 mM are shown in Figs. 5A and 5B, respectively. The high-q bump with a shoulder in the 50 mM SAXS data is characteristic for core-shell structures, whereas the $I \simeq q^{-3}$ power law trend in the low-q region is indicative of aggregation behaviour. Those micelle-like aggregates with a core-shell structure interact with each other, which is indicated by the presence of the structure factor peak at $q_S \simeq 0.03\,nm^{-1}$ in the mid-q range.

With increasing polymer concentration (decreasing the binding ratio of surfactants to polymers), the first minimum of the form-factor at $q \simeq 1\,nm^{-1}$ consistently shifts towards the higher q value, indicative of changes in the micelle structure, as compared to the pure SDS solution. It should be noted that above the *cmc* free micelles could be present in the solution and contribute significantly to scattering. The only sample, where this contribution is prominent, is composed of 500 ppm of the polymer and 50 mM of SDS.

At the lowest polymer concentration $c_{PVP} = 500\,ppm$, the SAXS profile for the sample containing 50 mM SDS is very similar to that of the pure micellar solution. The fitting parameters are similar to those of SDS micelles, with around 30 mM of the surfactant participating in the formation of micelles and 12 mM bound in elongated micelle-like aggregates, similar to the observation at [SDS] = 10 mM.

Furthermore, the aggregation number of the aggregates bound to the polymer $N_{agg}^b = 44$ is only slightly smaller than that of free SDS micelles, i.e. $n_{agg} = 49$. This implies that the polymer-bound aggregates were similar in shape but more compact compared to native surfactant micelles, possibly due to the penetration of hydrophobic grafts of the polymer into the micelle core.

At 10 mM SDS concentration, which corresponds to the decreased amount of bound surfactant, polymer-surfactant aggregates maintained a similar core-shell structure, but exhibited a mid-q slope of $q^{-1}$, which is indicative of an elongated structure, such as cylinders or elongated ellipsoids. The mid-q bump has a significantly smaller intensity, as compared to the complexes with 50 mM SDS, indicating reduced shell contrast due to a lower packing density of the surfactant headgroups.

Additionally, all 10 mM SDS SAXS curves exhibited $I \simeq q^{-1}$ at the higher q-range, which is attributed to the scattering from small amounts of polymer Gaussian chains. In order to take this into account, the contribution from the polymer chains with an excluded volume was added. Assuming limited swelling of the polymer in the vicinity of the micelle shell, the Flory exponent $\nu = 0.5$ was used.

Samples with $c_{PVP}$ = 500 ppm and 5000 ppm in the presence of 10 mM of SDS exhibited significant low-q scattering, attributed to aggregation, whereas such a behaviour was not observed for $c_{PVP}$ = 10000 and 20000 ppm which corresponds to 1 wt% and 2 wt% polymer concentration, respectively. Consequently, the SAXS data were fitted with two different models to account for the presence of low-q scattering and contributions of polymer chains. For $c_{PVP}$ = 500 and 5000 ppm, contributions from both the chains and from the power law were added to the cylindrical form-factor, whereas for $c_{PVP}$ = 10000 ppm and 20000 ppm only the term responsible for the scattering of the Gaussian chains together with the form-factor of core-shell ellipsoids was included into the calculations of total intensity (cf. Supplementary material, Figure S7).

Both ellipsoidal and cylindrical models were tested to describe the SAXS profiles for all polymer concentrations. The ellipsoidal model yielded unphysical dimensions of the hydrocarbon core at lower polymer concentrations, i.e. $R_{core} = 2.5$ Å (radius of a saturated hydrocarbon chain is about $r_{CH_2} = 2.81$ Å [66]) with an eccentricity $\epsilon = 40$; whereas at higher polymer concentration, where the aggregates are less

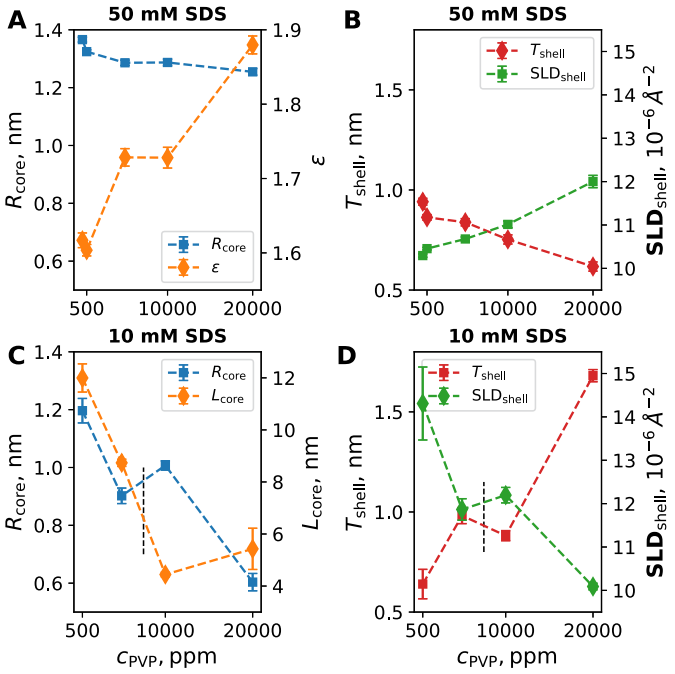


**Fig. 6.** SAXS fitting parameters of the aggregates extracted from the model. A. Radius and ellipticity of the aggregate core in the presence of 50 mM of SDS; B. Thickness and scattering length density of the aggregate shell in the presence of 50 mM of SDS; C. Radius and length of the aggregate core in the presence of 10 mM of SDS. Broken line indicates border between cylindrical (lower concentrations) and ellipsoidal models (higher concentrations); D. Thickness and scattering length density of the aggregate shell in the presence of 10 mM of SDS. Broken line indicates border between cylindrical (lower concentrations) and ellipsoidal models (higher concentrations). Where not visible, errors are comparable to, or smaller than, the data symbol size, with the error values listed in Supplementary material section S13.

elongated and more compact overall, the errors from the cylindrical model produced fits were significantly higher ($\chi^2_{cyl} = 18$ compared to $\chi^2_{ell} = 1.78$).

The fitting parameters to the models described above are shown in Fig. 6. A feature observed with increasing polymer concentration is the elongation of the aggregate core, corresponding to an increase in ellipticity. This is consistent with the decreased average polymer-surfactant binding, as the amount of surfactant per polymer chain decreased as was shown for the strongly interacting PSS/DTAB complexes [67]. Furthermore, the aggregate shell density increased accompanied by a decrease in its thickness. This indicates the incorporation of a significant amount of the polymer and counterions into the micelle headgroup region, leading to the displacement of water.

A different trend was observed for the samples with 10 mM SDS present in the solution, where the shell density decreased with the increase in polymer concentration, mostly due to the fact that the aggregation number of the complexes decreased, therefore fewer surfactant headgroups were available to fill the volume in the shell. Additionally, the longer axis of the core significantly decreased from ca. 12 nm in the presence of 500 ppm of the polymer down to 4 nm in the presence of 20000 ppm of the polymer.

Results of the SAXS data analysis indicate that the displacement of hydration water from the headgroup region is the consequence of the surfactant binding to the polymer and elongation of the aggregates upon increased binding below surfactant's *cmc*.

We have explored the possibility of varying the hydrocarbon core density in data fitting in order to gain an understanding of the effect of the incorporation of the hydrophobic grafts of the polymer on the size and density of the core, but this attempt produced very high core density with unphysical 70% hydration. Thus, the core density was fixed.

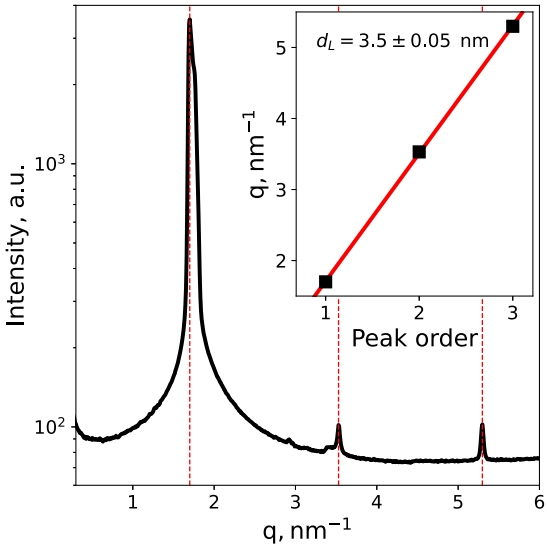


**Fig. 7.** SAXS curve of a PVP/SDS precipitate in excess water. Dashed red lines indicate the peak positions. Inset shows the peak positions in q, plotted against the diffraction order. Error bars are smaller than the symbol size and the solid line indicates the least square fit to the points.

Our fitting thus suggests that, at the highest surfactant concentration, aggregates were similar in shape to the free micelles which were only slightly perturbed by the insertion of hydrophobic grafts of the polymer into the core.

### 3.5. Structure of polymer-surfactant precipitates at pH = 2

At pH = 2 PVP is charged and electrostatic interactions between the polymer and the surfactant would drive the formation of precipitates The SAXS profile of the precipitate formed indicates the presence of a lamellar phase, as shown in the Fig. 7. In the inset, peak position q is plotted against the peak diffraction order, with a straight line representing the linear fit to the points, which gives a value of the lamellar spacing $d_L = 3.5 \pm 0.05$ nm.

Assuming that the two hydrocarbon chains of the SDS bilayer are in an all-trans conformation (using $d = 2.54$ Å $= 0.254$ nm for a length of two $CH_2$ units) and an overlap at 25% of their length due to interdigitation, the thickness of the bilayer hydrophobic part can be estimated as $d_H = (12 \cdot 0.254) \cdot 0.75 = 2.286 \simeq 2.3$ nm. It is widely accepted that for SDS the area of the headgroup is smaller than the cross section of the alkyl chain, therefore the maximum area per headgroup is approximated by that of 1-dodecanol $A = 24.86$ Å$^2$ reported by Legrand et al. [66].

Therefore, the thickness of the lamellae, incorporating the 2 headgroups, polymer chain and hydration water, equals to the 1.2 nm, leading to a volume $V_{tot} = A \cdot (d_L - d_H) = 24.86 \cdot (35 - 23) = 298$Å$^3$ per two surfactant molecules.

Molecular volumes of an SDS headgroup ($V_{head}$) and a PVP segment ($V_{PVP}$) were used to calculate the hydration water volume as $V_{H_2O} = V_{tot} - 2 \cdot V_{head} - V_{PVP} = 298 - 2 \cdot 59.8 - 148 = 30.4$Å$^2$, which is the molecular volume of just a single water molecule, and therefore the aggregates are highly dehydrated, despite being submerged in water.

The width of the first order of the diffraction peak can be used to estimate the number of layers contributing to the scattering. The size of the coherent scattering domain $D$ was calculated using Scherrer equation $D = \frac{2K\pi}{\Delta q}$, where $\Delta q$ is the full width at half maximum (FWHM) of the reflection peak, and $K = 0.88$ is the Scherrer constant for the 1D stack of reflecting planes. [68] This yields $D = 59$ nm, corresponding to $n_L = \frac{D}{d_L} = \frac{59}{3.5} = 16.86 \simeq 17$ bilayers.

As discussed in the section 3.4, SDS and PVP at pH = 9 form core-shell micelle-like structures even at surfactant concentrations below the cmc of the pure SDS. When PVP is neutral and hydrophobic forces are predominant, the complexes remain soluble and do not precipitate. At pH = 2, PVP moieties are protonated, and the interaction between PVP and SDS is dominated by the strong electrostatic attraction, leading to precipitation. Bastardo et al. [69] reported that complexes of SDS and hyperbranched poly(ethyleneimine) were reorganized into highly ordered structures as the amine group protonation at lower pH led to increased attractions between flat aggregates of polymer and surfactant which induced highly compact lamellar stacking. [70]. This is in line with our observation of water-poor precipitate formation at pH = 2 due to strong electrostatic interactions between PVP and SDS.

### 3.6. Driving forces for aggregate formation

The Gibbs energy of SDS aggregation can be decomposed into three components,

$$\Delta G^0_{tot} = \Delta G^0_h + \Delta G^0_e + \Delta G^0_{pol}. \quad (2)$$

where $\Delta G^0_h$ corresponds to the contribution of hydrophobic forces and tends to be negative, $\Delta G^0_e$ is due to the electrostatic repulsion between like-charged headgroups (therefore, positive) and $\Delta G^0_{pol}$ arises from the surfactant-polymer interaction which depends on the nature of the polymer moieties, concentration, and pH.

We can estimate the Gibbs energy of incorporating an SDS molecule into a micelle near the cmc as $\Delta G^0_{m,T=298\,\mathrm{K}} = (1+(1-\beta))\,RT \ln \mathrm{cmc} = -21.2\,\mathrm{kJ/mol} = -8.56\,\mathrm{kT}$. [71] In this equation, $\beta$ corresponds to the degree of ionization determined by SAXS, therefore $(1-\beta)$ corresponds to the fraction of counterions condensed on the micelles, and the value of SDS cmc was taken as 8 mM. It has been previously reported that, for SDS adsorption into the liquid-like surface monolayer, $\Delta G^0_{liq} = -19.67\,\mathrm{kT}$, which corresponds to the hydrophobic contribution. The total Gibbs energy for adsorption was $\Delta G^0_{ads} = -9.5\,\mathrm{kT}$, calculated as $\Delta G^0_{ads} = -\mathrm{kT} \ln K(\Gamma)$, where $K$ is the equilibrium adsorption constant includes both hydrophobic and electrostatic contributions. [72]

When the contribution from the polymer chains $\Delta G^0_{pol}$ is negative, $\Delta G^0_{tot}$ is further reduced, which would lead to an increase in the aggregation number at the same surfactant concentration. However, PVP is neutral at pH = 9; therefore, its contribution is attributed to the presence of hydrophobic grafts, entropic effects, or polarization of the PVP group induced by a nearby charged headgroup.

Further insights may be gained by considering surfactant binding above the polymer saturation concentration $c_{\mathrm{cac}}$. In Fig. 8, the aggregation number $N_{agg}$ calculated from the SAXS measurements is plotted vs. surfactant-to-polymer-ratio $\xi$ on a linear-log scale, with the dashed line indicating a 1:1 ratio between the two values.

For the surfactant concentration below the cmc of SDS and polymer saturation concentration ($\xi_{\mathrm{cac}}$), the increase in the aggregation number follows the mixing ratio $\xi$ linearly. At higher SDS concentration, [SDS] = 50 mM, the equilibrium is established between micelles and polymer chains, with the SDS aggregate dimensions close to those of free micelles, as shown in Fig. 6.

According to Lissi and Abuin [73], binding of micelle-like aggregates to the PVP chain is independent of polymer concentration and molecular weight. With PVP of a similar molecular weight to the one used in this work, polymer saturation (when all polymer chains accommodate at least one aggregate) occurred at 30 mM of SDS, with one SDS aggregate ($N_{agg} = 28 \pm 6$) formed every 76 PVP monomer units.

This is overall consistent with our observations; in our case, the SDS concentration was higher at 50 mM and the number of SDS molecules in the aggregate was $N_{agg} = 44 \pm 2$ for all polymer concentrations, as estimated by SAXS modelling. This difference arises from stimulated surfactant binding by the presence of hydrophobic grafts, which reduces $\Delta G^0_{pol}$ via recruiting additional surfactant molecules into the aggregates.

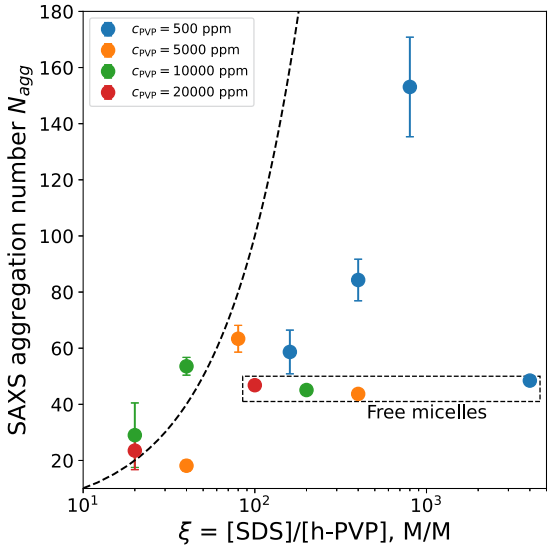


**Fig. 8.** Aggregation number $N_{agg}$, determined from SAXS of the PVP-SDS aggregates plotted against molar ratio $\xi$. The dashed line indicates the 1:1 ratio between the surfactant-to-polymer ratio and the aggregation number, i.e. $N_{agg} = \xi$.

At $c_{\mathrm{PVP}} = 500\,\mathrm{ppm}$ the critical association concentration $c_{\mathrm{cac}}^{500\,\mathrm{ppm}}$ is lower than the cmc of SDS, and the $N_{agg}$, determined by SAXS continued to increase with the surfactant concentration after the $c_{\mathrm{cac}}^{500\,\mathrm{ppm}}$. This behaviour resembles the formation of worm-like micelles in the presence of an electrolyte [74], as the hydrophobic contribution to the driving force overcomes the electrostatic repulsion contribution. This is consistent with a previous observation that after polymer saturation the mean aggregation number of the aggregates continued to increase [73]. This is due to the fact that the dodecyl sulfate anion is capable of inducing polarization of the PVP chain, thus allowing the chain to partially neutralize the effective charge of the surfactant molecule, leading to the reduced electrostatic repulsion [12]. The aggregates however retained colloidal stability because the neutralization was incomplete and they remained partially charged.

In summary, the primary driving force for aggregation is the hydrophobic attraction between the surfactant tails and the hydrophobic grafts of the polymer, but formation of larger aggregates is aided by the partial neutralization of the headgroup charge by the polarized PVP groups, which are present in the headgroup region of the micelles, as observed by SANS with contrast matching [38]. This is in accordance with observations in this work.

This is consistent with the behaviour of the surface tension isotherm, shown in Fig. 2. With increasing surfactant concentration, the polymer hydrophobic grafts are incorporated into the surfactant aggregates formed around the polymer and the headgroup charge is partially neutralized by the PVP groups. This suppresses polymer adsorption to the air-water interface, which is manifested in a gradual increase in the surface tension below $\xi = c_{\mathrm{cac}}$, indicated by the dashed line in the inset in Fig. 2. After the polymer saturation concentration $c_{\mathrm{cac}}$, added surfactants can be incorporated into the aggregates already formed instead of forming new polymer-associated aggregates. This leads to an increase in the aggregation number of the P-S complexes after $c_{\mathrm{cac}}$, as shown in Fig. 8, demonstrating that the mean aggregation number consistently increases with the surfactant-to-polymer ratio, with the exception of the samples with 50 mM of SDS, where the equilibrium is established with free SDS micelles bound to the polymer, rather than with individual surfactant molecules.

### 3.7. A model of the aggregation process

As discussed in the sections 3.4 and 3.6, at high pH, where PVP is deprotonated and therefore largely neutral, SDS forms aggregates to-

gether with the hydrophobically modified PVP even at concentration lower than cmc, for which the main driving force is the hydrophobic interaction.

From our surface tension measurement in Fig. 2 and SAXS data analysis in Fig. 8, we can describe the evolution of P-S aggregate structure with the surfactant concentration. Initially at extremely low surfactant concentration ([SDS] < 1 mM), no well-defined structures are formed, but the change in the surface tension of the mixture indicates polymer-surfactant interaction in operation. This change is attributed to the competitive adsorption of the polymer and surfactant on the interface and the cooperative interaction in the bulk solution. This means that at low surfactant concentration, formation of a P-S aggregate is favoured over adsorption at the interface, which leads to the formation of the relatively monodisperse P-S aggregates at surfactant concentrations below cmc.

The average number of molecules participating in the formation of these aggregates linearly increases with the surfactant-to-polymer ratio, as indicated in Fig. 8. Such a behaviour is consistent with the predictions of the Closed Association (CA) model, which states that the formation of P-S aggregates with the same aggregation number and the average amount of bound surfactant is increased by the increasing number of polymer chains participating in the formation of aggregates. In our observation, this is manifested as the increase in surface tension below $c_{cac}$, as more and more polymer chains are drawn away from the surface.

When all polymer grafts are engaged in aggregate formation after $c_{cac}$, the surface tension drops sharply and the average aggregation number of the P-S aggregates increases simultaneously, as the $\Delta G^0_{mic} = -8.56\,kT$ is still higher than $\Delta G^0_{agg}$ of incorporating a surfactant molecule into the aggregate. This corresponds to the Zimm-Bragg association model, which is based on the assumption of cooperative adsorption of the surfactant to the polymer, i.e. incorporating new surfactant molecules into existing aggregates. Our observations are coherent with other studies available in the literature [15,67,75], where special attention was necessary for sample preparation to avoid the formation of out-of-equilibrium structures, so that the local surfactant concentration never exceeded the precipitation threshold.

We suggest that the above complexation mechanism holds for equilibrium P-S complexation in the absence of free micelles. Compared to a previous study where the equilibrium complexes were obtained through careful sample preparation [67], for our system it was achieved by suppressing electrostatic forces, with the hydrophobic effect acting as the driving force between the hydrophobically modified PVP and SDS, thus allowing for a reorganization of the P-S complexes. At pH = 2, when the electrostatic interaction is dominant, once the surfactant molecule is bound to a polymer, its mobility is hindered and the solid precipitate is formed as discussed in section 3.5. This suggests that the interaction between SDS and h-PVP is strongly dependent on the external factors, such as pH and ionic strength. This can be rationalized in the context of the competition between solvent and polymer to be in the close vicinity of the surfactant headgroup. It points to the possibility for tuning the polymer-surfactant interaction in the modified or non-aqueous solvent environments.

## 4. Conclusion

Whilst out-of-equilibrium polymer-surfactant aggregates formed due to the strong electrostatic interaction have been previously studied [26–28], challenges remained to experimentally obtain equilibrium P-S complexes. As a result, our understanding of how the polymer charge tunability affects surfactant binding and the complex structure remains incomplete. Here, the structure of P-S complexes in solution with the driving force switchable between hydrophobic and electrostatic interactions has been investigated, enabled by use of PVP with a pH-tuneable charge and hydrophobic grafts along the backbone.

Combining SAXS data fitted on the absolute intensity scale with surface tension experiments has allowed us to gain a mechanistic insight into the binding mechanism and elucidate the role of hydrophobic interaction in the formation of P-S aggregates at pH = 9 when the polymer is neutral. Under these conditions and above a certain critical association surfactant concentration, which is a function solely of the surfactant-to-polymer ratio, we have found micelle-like aggregates of SDS with PVP chains incorporated into the headgroup regions. These aggregates grow in size with increasing surfactant concentration and abruptly change shape after the formation of surfactant micelles. Linear dimensions of these aggregates are limited by the contour length of the polymer, which stabilizes the aggregates by decreasing electrostatic repulsion between surfactant heads.

At pH = 2, the PVP is charged and we have observed a transformation of core-shell ellipsoidal aggregates into highly ordered water-poor lamellar precipitates. We have estimated that only a single water molecule per two surfactants is present in the precipitate. This suggests the displacement of hydration water in the surfactant headgroup region by the polymer moieties upon increase in the interaction strength.

Our results contribute to the fundamental understanding of the driving forces of polymer-surfactant co-assembly and the role of hydrophobic interaction, relevant to the rational design of product formulations in which polymer-surfactant complexes are widespread. Furthermore, our results lay the ground for further work on potentially tuning the polymer-surfactant interaction in the modified or non-aqueous solvent environments.

## CRediT authorship contribution statement

**Egor A. Bersenev:** Writing – original draft, Methodology, Investigation, Formal analysis, Conceptualization. **Lauren Matthews:** Writing – review & editing, Investigation. **Valentina Rein:** Writing – review & editing. **Rebecca J. Fong:** Writing – review & editing, Resources. **Oleg V. Konovalov:** Writing – review & editing, Supervision, Resources, Funding acquisition, Conceptualization. **Wuge H. Briscoe:** Writing – review & editing, Supervision, Funding acquisition, Conceptualization.

## Declaration of competing interest

The authors declare that they have no known competing financial interests or personal relationships that could have appeared to influence the work reported in this paper.

## Acknowledgements

The authors would like to acknowledge Beatrice Barletti and Laura Mateo Minarro for their assistance during SAXS experiment. Beamline staff of ID02 is acknowledged for their perfect technical support. Dr. Martin Rosenthal is thanked for the provided beamtime on BM26 DUBBLE (ESRF) and his assistance during measurements. The authors thank Holly Stockdale for her assistance in the NMR characterisation of the polymer. E.A.B. would like to thank Dr. Eva Zilber for proofreading the manuscript. ESRF is acknowledged for the provision of beamtime under proposal SC-5448. Partnership for Soft Condensed Matter is acknowledged for the provision of laboratory facilities for the sample preparation and tensiometry experiments. E.A.B. has received funding from the InnovaXN doctoral training program supported by the European Union's Horizon 2020 research and innovation program under the Marie Skłodowska-Curie grant agreement 847439.

## Appendix A. Supplementary material

Supplementary material related to this article can be found online at https://doi.org/10.1016/j.jcis.2025.137572.

## Data availability

Data are available at the ESRF repository with no restrictions and are referenced in the manuscript.

## References


[1] C.D. Bain, P.M. Claesson, D. Langevin, R. Meszaros, T. Nylander, C. Stubenrauch, S. Titmuss, R. von Klitzing, Complexes of surfactants with oppositely charged polymers at surfaces and in bulk, Adv. Colloid Interface Sci. 155 (1) (2010) 32–49, https://doi.org/10.1016/j.cis.2010.01.007.

[2] L. Fernández-Peña, I. Abelenda-Nuñez, M. Hernández-Rivas, F. Ortega, R.G. Rubio, E. Guzmán, Impact of the bulk aggregation on the adsorption of oppositely charged polyelectrolyte-surfactant mixtures onto solid surfaces, Adv. Colloid Interface Sci. 282 (2020) 102203, https://doi.org/10.1016/J.CIS.2020.102203.

[3] E.D. Goddard, Polymer/surfactant interaction: interfacial aspects, J. Colloid Interface Sci. 256 (1) (2002) 228–235, https://doi.org/10.1006/JCIS.2001.8066.

[4] P.A. Cornwell, A review of shampoo surfactant technology: consumer benefits, raw materials and recent developments, Int. J. Cosmet. Sci. 40 (1) (2018) 16–30, https://doi.org/10.1111/ics.12439.

[5] E. Guzmán, Polyelectrolyte-surfactant mixtures as the model for understanding the performance of 2-in-1 shampoo formulations, Curr. Cosmet. Sci. 1 (1) (2022) 41–50, https://doi.org/10.2174/2666779701666220211145354.

[6] M. Gradzielski, Polymer–surfactant interaction for controlling the rheological properties of aqueous surfactant solutions, Curr. Opin. Colloid Interface Sci. 63 (2023) 101662, https://doi.org/10.1016/j.cocis.2022.101662.

[7] A. Bureiko, A. Trybala, N. Kovalchuk, V. Starov, Current applications of foams formed from mixed surfactant–polymer solutions, Adv. Colloid Interface Sci. 222 (2015) 670–677, https://doi.org/10.1016/j.cis.2014.10.001.

[8] B.M. Folmer, B. Kronberg, Effect of surfactant-polymer association on the stabilities of foams and thin films: sodium dodecyl sulfate and poly(vinyl pyrrolidone), Langmuir 16 (14) (2000) 5987–5992, https://doi.org/10.1021/la991655k.

[9] L. Chiappisi, S. Prévost, I. Grillo, M. Gradzielski, From crab shells to smart systems: chitosan-alkylethoxy carboxylate complexes, Langmuir 30 (35) (2014) 10615–10616, https://doi.org/10.1021/la502569p.

[10] Z. Draelos, S. Hornby, R.M. Walters, Y. Appa, Hydrophobically modified polymers can minimize skin irritation potential caused by surfactant-based cleansers, J. Cosmet. Derm. 12 (4) (2013) 314–321, https://doi.org/10.1111/jocd.12061.

[11] M.J. Fevola, R.M. Walters, J.J. LiBrizzi, A new approach to formulating mild cleansers: hydrophobically-modified polymers for irritation mitigation, in: Polymeric Delivery of Therapeutics, in: ACS Symposium Series, vol. 1053, American Chemical Society, 2010, pp. 221–242.

[12] K. Chari, The structure of the PVP-SDS complex in water, J. Colloid Interface Sci. 151 (1) (1992) 294–296, https://doi.org/10.1016/0021-9797(92)90259-O.

[13] P. Hansson, Self-assembly of ionic surfactants in polyelectrolyte solutions: a model for mixtures of opposite charge, Langmuir 17 (14) (2001) 4167–4180, https://doi.org/10.1021/la010390i.

[14] I. Satake, J.T. Yang, Interaction of sodium decyl sulfate with poly(L-ornithine) and poly(L-lysine) in aqueous solution, Biopolymers 15 (11) (1976) 2263–2275, https://doi.org/10.1002/bip.1976.360151113.

[15] R. Mészáros, L. Thompson, M. Bos, I. Varga, T. Gilányi, Interaction of sodium dodecyl sulfate with polyethyleneimine: surfactant-induced polymer solution colloid dispersion transition, Langmuir 19 (3) (2003) 609–615, https://doi.org/10.1021/la026616e.

[16] A. Mezei, K. Pojják, R. Mészáros, Nonequilibrium features of the association between poly(vinylamine) and sodium dodecyl sulfate: the validity of the colloid dispersion concept, J. Phys. Chem. B 112 (32) (2008) 9693–9699, https://doi.org/10.1021/jp802196c.

[17] R.A. Campbell, M. Yanez Arteta, A. Angus-Smyth, T. Nylander, I. Varga, Multilayers at interfaces of an oppositely charged polyelectrolyte/surfactant system resulting from the transport of bulk aggregates under gravity, J. Phys. Chem. B 116 (27) (2012) 7981–7990, https://doi.org/10.1021/jp304564x.

[18] I. Varga, R.A. Campbell, General physical description of the behavior of oppositely charged polyelectrolyte/surfactant mixtures at the air/water interface, Langmuir 33 (23) (2017) 5915–5924, https://doi.org/10.1021/acs.langmuir.7b01288.

[19] P.L. Dubin, D.R. Rigsbee, L.M. Gan, M.A. Fallon, Equilibrium binding of mixed micelles to oppositely charged polyelectrolytes, Macromolecules 21 (8) (1988) 2555–2559, https://doi.org/10.1021/ma00186a040.

[20] P. Bahadur, P. Dubin, Y.K. Rao, Complex formation between sodium dodecyl sulfate and poly(4-vinylpyridine N-oxide), Langmuir 11 (6) (1995) 1951–1955, https://doi.org/10.1021/la00006a021.

[21] A. Mezei, R. Mészáros, Novel nanocomplexes of hyperbranched poly(ethyleneimine), sodium dodecyl sulfate and dodecyl maltoside, Soft Matter 4 (3) (2008) 586–592, https://doi.org/10.1039/B715754A.

[22] S. Peng, C. Wu, Surfactant effect on pH and temperature sensitivities of poly(N-vinylcaprolactam-co-sodium acrylate) microgels, Macromolecules 34 (3) (2001) 568–571, https://doi.org/10.1021/ma0009909.

[23] M.S. Babaev, A.N. Lobov, N.M. Shishlov, S.V. Kolesov, pH-sensitive particles of polymer-surfactant complexes based on a copolymer of N,N'-diallyl-N,N'-dimethylammonium chloride with maleic acid and sodium dodecyl sulfate, React. Funct. Polym. 178 (2022) 105359, https://doi.org/10.1016/j.reactfunctpolym.2022.105359.

[24] L. Braun, M. Uhlig, O. Löhmann, R.A. Campbell, E. Schneck, R. von Klitzing, Insights into extended structures and their driving force: influence of salt on polyelectrolyte/surfactant mixtures at the air/water interface, ACS Appl. Mater. Interfaces 14 (23) (2022) 27347–27359, https://doi.org/10.1021/acsami.2c04421.

[25] J. Carrascosa-Tejedor, A. Tummino, B. Fehér, A. Kardos, M. Efstratiou, M.W.A. Skoda, P. Gutfreund, A. Maestro, M.J. Lawrence, R.A. Campbell, I. Varga, Effects of charge density on spread hyperbranched polyelectrolyte/surfactant films at the air/water interface, Langmuir 39 (42) (2023) 14869–14879, https://doi.org/10.1021/acs.langmuir.3c01514.

[26] N. Péron, R. Mészáros, I. Varga, T. Gilányi, Competitive adsorption of sodium dodecyl sulfate and polyethylene oxide at the air/water interface, J. Colloid Interface Sci. 313 (2) (2007) 389–397, https://doi.org/10.1016/j.jcis.2007.04.031.

[27] K. Tonigold, I. Varga, T. Nylander, R.A. Campbell, Effects of aggregates on mixed adsorption layers of poly(ethylene imine) and sodium dodecyl sulfate at the air/liquid interface, Langmuir 25 (7) (2009) 4036–4046, https://doi.org/10.1021/la8028325.

[28] R. Mészáros, The thermodynamic stability of the mixtures of hyperbranched poly(ethyleneimine) and sodium dodecyl sulfate at low surfactant-to-polyelectrolyte ratios, J. Colloid Interface Sci. 338 (2) (2009) 444–449, https://doi.org/10.1016/j.jcis.2009.06.053.

[29] X. Zhang, D. Taylor, R. Thomas, J. Penfold, I. Tucker, Modifying the adsorption properties of anionic surfactants onto hydrophilic silica using the pH dependence of the polyelectrolytes PEI, ethoxylated PEI, and polyamines, Langmuir 27 (7) (2011) 3569–3577, https://doi.org/10.1021/la1046723.

[30] H. Comas-Rojas, G. Fernández-Catá, K.J. Edler, S.J. Roser, A. Pérez-Gramatges, Multiple thin film formation from dilute mixtures of polyethyleneimine (PEI) and cetyltrimethylammonium bromide (CTAB), J. Colloid Interface Sci. 339 (2) (2009) 495–501, https://doi.org/10.1016/j.jcis.2009.07.067.

[31] P. Li, J. Penfold, R.K. Thomas, H. Xu, Multilayers formed by polyelectrolyte-surfactant and related mixtures at the air-water interface, Adv. Colloid Interface Sci. 269 (2019) 43–86, https://doi.org/10.1016/J.CIS.2019.04.002.

[32] I.P. Purcell, J.R. Lu, R.K. Thomas, A.M. Howe, J. Penfold, Adsorption of sodium dodecyl sulfate at the surface of aqueous solutions of poly(vinylpyrrolidone) studied by neutron reflection, Langmuir 14 (7) (1998) 1637–1645, https://doi.org/10.1021/la971161s.

[33] M. Prasad, R. Palepu, S.P. Moulik, Interaction between sodium dodecyl sulfate (SDS) and polyvinylpyrrolidone (PVP) investigated with forward and reverse component addition protocols employing tensiometric, conductometric, microcalorimetric, electrokinetic, and DLS techniques, Colloid Polym. Sci. 284 (8) (2006) 871–878, https://doi.org/10.1007/s00396-005-1453-8.

[34] M.J. Blandamer, B. Briggs, P.M. Cullis, K.D. Irlam, J.B.F.N. Engberts, J. Kevelam, Titration microcalorimetry of adsorption processes in aqueous systems, J. Chem. Soc., Faraday Trans. 94 (2) (1998) 259–266, https://doi.org/10.1039/A704667G, publisher: the Royal Society of Chemistry.

[35] R. Feng, M. Chen, Y. Fang, Y. Fan, Y. Xia, Supramolecular interactions in the pseudo-polyanions of polyvinylpyrrolidone complexed with various anionic surfactants, Colloids Surf. A, Physicochem. Eng. Asp. 671 (2023) 131585, https://doi.org/10.1016/j.colsurfa.2023.131585.

[36] Y. Wu, J. Chen, Y. Fang, M. Zhu, Polyvinylpyrrolidone-sodium dodecylsulfate complex is a family of pseudo-polyanions with different charge densities: evidence from capillary electrophoresis, capillary viscosimetry and conductometry, J. Colloid Interface Sci. 479 (2016) 34–42, https://doi.org/10.1016/j.jcis.2016.06.037.

[37] P. Roscigno, F. Asaro, G. Pellizer, O. Ortona, L. Paduano, Complex formation between poly(vinylpyrrolidone) and sodium decyl sulfate studied through NMR, Langmuir 19 (23) (2003) 9638–9644, https://doi.org/10.1021/la034928r, publisher: American Chemical Society.

[38] P.C. Griffiths, N. Hirst, A. Paul, S.M. King, R.K. Heenan, R. Farley, Effect of ethanol on the interaction between poly(vinylpyrrolidone) and sodium dodecyl sulfate, Langmuir 20 (16) (2004) 6904–6913, https://doi.org/10.1021/la049348o, publisher: American Chemical Society.

[39] G. Mangiapia, D. Berti, P. Baglioni, J. Teixeira, L. Paduano, Structural investigation on the poly(vinylpyrrolidone)-water system in the presence of sodium decyl sulfate and sodium decanesulfonate: a small angle neutron scattering study, J. Phys. Chem. B 108 (28) (2004) 9772–9779, https://doi.org/10.1021/jp0495388, publisher: American Chemical Society.

[40] Y.J. Nikas, D. Blankschtein, Complexation of nonionic polymers and surfactants in dilute aqueous solutions, Langmuir 10 (10) (1994) 3512–3528, https://doi.org/10.1021/la00022a026, publisher: American Chemical Society.

[41] Y. Wu, M. Chen, Y. Fang, W. Wang, Investigation of pseudo-polyanion formation between polyvinylpyrrolidone and sodium dodecanoate in aqueous solution by capillary electrophoresis, conductometry, tensiometry and calcium stability, RSC Adv. 7 (15) (2017) 9338–9346, https://doi.org/10.1039/C6RA26629K.

[42] S. Demirci, A. Alaslan, T. Caykara, Preparation, characterization and surface pKa values of poly(N-vinyl-2-pyrrolidone)/chitosan blend films, Appl. Surf. Sci. 255 (11) (2009) 5979–5983, https://doi.org/10.1016/j.apsusc.2009.01.050.

[43] T. Narayanan, M. Sztucki, T. Zinn, J. Kieffer, A. Homs-Puron, J. Gorini, P. Van Vaerenbergh, P. Boesecke, Performance of the time-resolved ultra-small-angle x-ray scattering beamline with the extremely brilliant source, J. Appl. Crystallogr. 55 (1) (2022) 98–111.

[44] E. Bersenev, B. Barletti, L. Mateo Minarro, L. Matthews, Balance of hydrophobic and electrostatic interaction of polymers and surfactants: case of anionic surfactant and hydrophobically modified polymer, https://doi.org/10.15151/ESRF-DC-1998386360, Sep. 2023.

[45] J. Yang, T. Sato, Micellar structure of a hydrophobically modified pullulan in an aqueous solution, Macromolecules 53 (18) (2020) 7970–7979, https://doi.org/10.1021/acs.macromol.0c01319.

[46] C.-C. Wang, L.-H. Lin, H.-T. Lee, Y.-W. Ye, Surface activity and micellization properties of chitosan-succinyl derivatives, Colloids Surf. A, Physicochem. Eng. Asp. 389 (1) (2011) 246–253, https://doi.org/10.1016/j.colsurfa.2011.08.017.
[47] O. Inta, R. Yoksan, J. Limtrakul, Hydrophobically modified chitosan: a bio-based material for antimicrobial active film, Mater. Sci. Eng. C 42 (2014) 569–577, https://doi.org/10.1016/j.msec.2014.05.076.
[48] D. Bolten, M. Türk, Experimental study on the surface tension, density, and viscosity of aqueous poly(vinylpyrrolidone) solutions, J. Chem. Eng. Data 56 (3) (2011) 582–588, https://doi.org/10.1021/je101277c, publisher: American Chemical Society.
[49] J. Águila Hernández, A. Trejo, B.E. García-Flores, Volumetric and surface tension behavior of aqueous solutions of polyvinylpyrrolidone in the range (288 to 303) K, J. Chem. Eng. Data 56 (5) (2011) 2371–2378, https://doi.org/10.1021/je101330b, publisher: American Chemical Society.
[50] P. Letellier, M. Turmine, Non-applicability of the Gibbs–Duhem relation in nonextensive thermodynamics. Case of micellar solutions, J. Phys. Chem. B 119 (10) (2015) 4143–4154, https://doi.org/10.1021/jp512576y.
[51] H. Arai, M. Murata, K. Shinoda, The interaction between polymer and surfactant: the composition of the complex between polyvinylpyrrolidone and sodium alkyl sulfate as revealed by surface tension, dialysis, and solubilization, J. Colloid Interface Sci. 37 (1) (1971) 223–227, https://doi.org/10.1016/0021-9797(71)90284-0.
[52] J. Penfold, I. Tucker, R.K. Thomas, J. Zhang, Adsorption of polyelectrolyte/surfactant mixtures at the air-solution interface: poly(ethyleneimine)/sodium dodecyl sulfate, Langmuir 21 (22) (2005) 10061–10073, https://doi.org/10.1021/la0505014.
[53] A. Slastanova, R.A. Campbell, T. Snow, E. Mould, P. Li, R.J.L. Welbourn, M. Chen, E. Robles, W.H. Briscoe, Synergy, competition, and the “hanging” polymer layer: interactions between a neutral amphiphilic ‘tardigrade’ comb co-polymer with an anionic surfactant at the air-water interface, J. Colloid Interface Sci. 561 (2020) 181–194, https://doi.org/10.1016/j.jcis.2019.11.017.
[54] A. Slastanova, R.A. Campbell, L. Islas, R.J.L. Welbourn, J.R.P. Webster, M. Vaccaro, M. Chen, E. Robles, W.H. Briscoe, Interfacial complexation of a neutral amphiphilic ‘tardigrade’ co-polymer with a cationic surfactant: transition from synergy to competition, J. Colloid Interface Sci. 606 (2022) 1064–1076, https://doi.org/10.1016/j.jcis.2021.08.014.
[55] D.J. Cooke, J.A.K. Blondel, J. Lu, R.K. Thomas, Y. Wang, B. Han, H. Yan, J. Penfold, Interaction between poly(ethylene oxide) and monovalent dodecyl sulfates studied by neutron reflection, Langmuir 14 (8) (1998) 1990–1995, https://doi.org/10.1021/la971129y.
[56] D.J. Cooke, C.C. Dong, J.R. Lu, R.K. Thomas, E.A. Simister, J. Penfold, Interaction between poly(ethylene oxide) and sodium dodecyl sulfate studied by neutron reflection, J. Phys. Chem. B 102 (25) (1998) 4912–4917, https://doi.org/10.1021/jp9804291.
[57] D.J.F. Taylor, R.K. Thomas, J.D. Hines, K. Humphreys, J. Penfold, The adsorption of oppositely charged polyelectrolyte/surfactant mixtures at the air/water interface: neutron reflection from dodecyl trimethylammonium bromide/sodium poly(styrene sulfonate) and sodium dodecyl sulfate/poly(vinyl pyridinium chloride), Langmuir 18 (25) (2002) 9783–9791, https://doi.org/10.1021/la020503d.
[58] H.G. Mortensen, J.K. Madsen, K.K. Andersen, T. Vosegaard, G.R. Deen, D.E. Otzen, J.S. Pedersen, Myoglobin and $\alpha$-lactalbumin form smaller complexes with the biosurfactant rhamnolipid than with SDS, Biophys. J. 113 (12) (2017) 2621–2633, https://doi.org/10.1016/j.bpj.2017.10.024.
[59] I.W. Hamley, V. Castelletto, Sodium dodecyl sulfate micelles: accurate analysis of small-angle X-ray scattering data through form factor and atomistic molecular dynamics modelling, Colloids Surf. A, Physicochem. Eng. Asp. 696 (2024) 134394, https://doi.org/10.1016/j.colsurfa.2024.134394.
[60] M. Bergström, J.S. Pedersen, Structure of pure SDS and DTAB micelles in brine determined by small-angle neutron scattering (SANS), Phys. Chem. Chem. Phys. 1 (18) (1999) 4437–4446, https://doi.org/10.1039/A903469B.
[61] J.S. Pedersen, P. Schurtenberger, Scattering functions of semiflexible polymers with and without excluded volume effects, Macromolecules 29 (23) (1996) 7602–7612, https://doi.org/10.1021/ma9607630.
[62] B. Hammouda, Analysis of the Beaucage model, J. Appl. Crystallogr. 43 (6) (2010) 1474–1478, https://doi.org/10.1107/S0021889810033856.
[63] G. Strobl, The physics of polymers, Polymer 15 (5) (2003), https://doi.org/10.1016/0032-3861(74)90120-7, ISSN 00323861, Springer Berlin, Heidelberg.
[64] M. Kamli, M. Guettari, T. Tajouri, Structure of polyvinylpyrrolidone in water/ethanol mixture in dilute and semi-dilute regimes: roles of solvents mixture composition and polymer concentration, J. Mol. Liq. 382 (2023) 122014, https://doi.org/10.1016/j.molliq.2023.122014.
[65] T. Sun, H.E. King, Aggregation behavior in the semidilute poly(N-vinyl-2-pyrrolidone)/water system, Macromolecules 29 (9) (1996) 3175–3181, https://doi.org/10.1021/ma951734c, publisher: American Chemical Society.
[66] J.F. Legrand, A. Renault, O. Konovalov, E. Chevigny, J. Als-Nielsen, G. Grübel, B. Berge, X-ray grazing incidence studies of the 2D crystallization of monolayers of 1-alcohols at the air-water interface, Thin Solid Films 248 (1) (1994) 95–99, https://doi.org/10.1016/0040-6090(94)90218-6.
[67] B. Fehér, A. Wacha, B. Jezsó, A. Bóta, J.S. Pedersen, I. Varga, The evolution of equilibrium poly(styrene sulfonate) and dodecyl trimethylammonium bromide supramolecular structure in dilute aqueous solution with increasing surfactant binding, J. Colloid Interface Sci. 651 (2023) 992–1007, https://doi.org/10.1016/j.jcis.2023.08.002.
[68] L.J. Fox, L. Matthews, H. Stockdale, S. Pichai, T. Snow, R.M. Richardson, W.H. Briscoe, Structural changes in lipid mesophases due to intercalation of dendritic polymer nanoparticles: swollen lamellae, suppressed curvature, and augmented structural disorder, Acta Biomater. 104 (2020) 198–209, https://doi.org/10.1016/j.actbio.2019.12.036.
[69] L.A. Bastardo, V.M. Garamus, M. Bergström, P.M. Claesson, The structures of complexes between polyethylene imine and sodium dodecyl sulfate in $D_2O$: a scattering study, J. Phys. Chem. B 109 (1) (2005) 167–174, https://doi.org/10.1021/jp046837o.
[70] M. Bergström, U.R.M. Kjellin, P.M. Claesson, J.S. Pedersen, M.M. Nielsen, A small-angle X-ray scattering study of complexes formed in mixtures of a cationic polyelectrolyte and an anionic surfactant, J. Phys. Chem. B 106 (44) (2002) 11412–11419, https://doi.org/10.1021/jp021008t.
[71] N.E. Olesen, P. Westh, R. Holm, Determination of thermodynamic potentials and the aggregation number for micelles with the mass-action model by isothermal titration calorimetry: a case study on bile salts, J. Colloid Interface Sci. 453 (2015) 79–89, https://doi.org/10.1016/j.jcis.2015.03.069.
[72] I. Varga, R. Mészáros, T. Gilányi, Adsorption of sodium alkyl sulfate homologues at the air/solution interface, J. Phys. Chem. B 111 (25) (2007) 7160–7168, https://doi.org/10.1021/jp071344f.
[73] E.A. Lissi, E. Abuin, Aggregation numbers of sodium dodecyl sulfate micelles formed on poly(ethylene oxide) and poly(vinyl pyrrolidone) chains, J. Colloid Interface Sci. 105 (1) (1985) 1–6, https://doi.org/10.1016/0021-9797(85)90340-6.
[74] G.V. Jensen, R. Lund, J. Gummel, T. Narayanan, J.S. Pedersen, Monitoring the transition from spherical to polymer-like surfactant micelles using small-angle X-ray scattering, Angew. Chem., Int. Ed. 53 (43) (2014) 11524–11528, https://doi.org/10.1002/anie.201406489.
[75] A. Abraham, A. Kardos, A. Mezei, R.A. Campbell, I. Varga, Effects of ionic strength on the surface tension and nonequilibrium interfacial characteristics of poly(sodium styrenesulfonate)/dodecyltrimethylammonium bromide mixtures, Langmuir 30 (17) (2014) 4970–4979, https://doi.org/10.1021/la500637v.